It's complicated: curvature, diffusion and lipid sorting within the two membranes of *Escherichia coli*

Pin-Chia Hsu,[1‡]Firdaus Samsudin,[1‡] Jonathan Shearer,[1] and Syma Khalid[1].*

[1]School of Chemistry, University of Southampton, Southampton, UK, SO17 1BJ.

AUTHOR INFORMATION

Corresponding Author

* S.Khalid@soton.ac.uk to whom correspondence should be addressed.

ABSTRACT The cell envelope of Gram-negative bacteria is composed of two membranes separated by a soluble region. Here, we report microsecond timescale coarse-grained molecular dynamics simulations of models of the *E. coli* cell envelope that incorporate both membranes and various native membrane proteins. Our results predict that both the inner and outer membranes curve in a manner dependent on the size of the embedded proteins. The tightly cross-linked lipopolysaccharide molecules (LPS) of the outer membrane cause a strong coupling between the movement of proteins and lipids. Whilst the flow of phospholipids is more random, their diffusion is nevertheless influenced by nearby proteins. Our results reveal protein-induced lipid sorting, whereby cardiolipin is significantly enriched within the vicinity of the water channel AqpZ and the multidrug efflux pump AcrBZ. In summary, our results provide unprecedented details of the intricate relationship between both membranes of *E. coli* and the proteins embedded within them.

TOC GRAPHIC

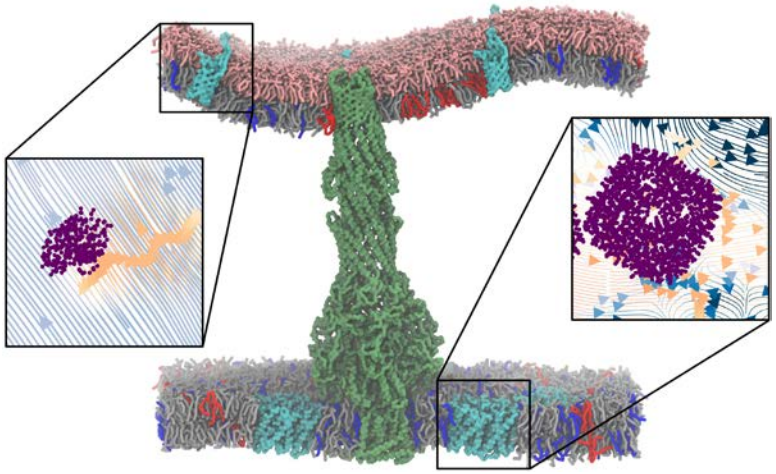

.

KEYWORDS bacterial membrane, molecular dynamics, diffusion, lipopolysaccharide, lipid enrichment

In Gram-negative bacteria, the envelope surrounding the cells is composed of an outer membrane (OM) made largely of lipopolysaccharide (LPS) in the outer leaflet and various species of phospholipids in the inner leaflet, an inner membrane (IM) containing only phospholipids, and a periplasm that accommodates the peptidoglycan cell wall.[1–4] Biological membranes are populated by numerous proteins at a concentration reaching as high as 25% area occupancy, resulting in crowded environments.[5,6] Over the last few years it has become increasingly apparent that lipids within biological membranes have an intricate relationship with membrane proteins.[7–11] Proteins can affect the physical properties of membranes such as stiffness and curvature,[12,13] and impede lipid diffusion,[14–16] while annular lipids found within 20 Å of a given protein diffuse together as a dynamic complex.[15]

The bacterial cell envelope accommodates proteins that traverse both the IM and OM, such as the multi-drug efflux pump AcrABZ-TolC,[17,18] which potentially influence the local dynamics of both membranes and surrounding proteins. Details of such effects are sparse due to the immense difficulties in performing experiments at high enough resolution and computational studies of such large systems. Here we employed coarse-grained methodologies to construct a model of the two membranes of *E. coli* held together by the AcrABZ-TolC complex, and populated with varying types and copy numbers of membrane proteins (Table 1, Table S1 and Fig S1). These copy numbers are equivalent to around 15-30% membrane area occupancy, which represent biologically relevant protein concentration.[5] We chose the aquaporin AqpZ[19] and lactose permease LacY[20] to include in the IM as they both are very well-studied integral IM proteins and represent two different protein sizes. The OM porin OmpA is one of the most ubiquitous OM

proteins in *E. coli*;[21] we therefore incorporate this protein into the OM in its two forms: i) the monomeric N-terminal β-barrel, and ii) the full-length homodimer with periplasmic globular domains[22–24].

Table 1: Summary of the composition of simulation systems

System	Time (μs)	OM		IM		
		TolC[c]	OmpA	AcrBZ[c]	AqpZ	LacY
1	2 x 10	Outer membrane only				
2	2 x 10	Inner membrane only				
3	2 x 10	1	4[a]	1	4	-
4	2 x 10	1	6[a]	1	6	-
5	2 x 10	1	8[a]	1	8	-
6	2 x 10	1	8[b]	1	-	8

[a]N-terminal domain of OmpA monomer

[b]Full length OmpA homodimer

[c]All systems contain the periplasmic subunit AcrA that connects the AcrBZ subunit in the IM to the TolC subunit in the OM

To measure the degree of membrane curvature, we employed the Helfrich-Canham elastic theory that models the membrane as a continuous elastic sheet and describes its stiffness by a bending rigidity constant (K_c) based on the variation in the height of the membrane surface,[12,25,26] here given by the positions of the phosphate beads throughout the simulations (Fig. 1). In the absence of any protein, the IM showed a small degree of curvature as evidenced by the large value of K_c,

which is comparable to the POPE/POPG model membrane.[12] Addition of 4 copies of AqpZ resulted in a substantial decrease in the K_c value, indicating that this protein can induce membrane curvature and deformations. Further addition of AqpZ, however, increased the stiffness of the membrane, with membrane containing 8 AqpZ showing a similar K_c value to the protein-free system. Interestingly, System 6 displayed the largest degree of bending in the IM despite having the same number of proteins as System 5, which could be attributed to LacY being significantly smaller than AqpZ. Together this suggests that integral IM proteins results in membrane curvature; this however is potentially dependent on the membrane surface area occupied by the proteins, whereby higher occupancy results in a stiffer membrane, similar to what has been observed in large-scale simulations of the plasma membrane.[27]

The OM remained almost perfectly flat throughout the entire 10 μs simulations without any protein, as indicated by the higher K_c value compared to the IM. The strong cross-links between adjacent LPS molecules in the outer leaflet potentially maintain the integrity of the membrane, preventing it from any structural deformations. Congruently increasing the number of OmpA monomers from System 3 to System 5 resulted in a gradual increase in the degree of membrane curvature, suggesting that these porins weakened the network of LPS-LPS interactions to allow the membrane to bend. The OM, however, became stiffer with the inclusion of the full-length OmpA dimer, perhaps due to the C-terminal periplasmic domain interacting with the inner leaflet[23,24] and therefore stabilizing the membrane. Overall, it is evident the degree of membrane curvature and deformation is dependent on the number and type of proteins present in the IM and OM.

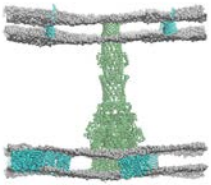

Fig 1. Membrane curvature and deformations in the IM and OM. (A) The power spectra of height fluctuations of the phosphate beads during the last 5 μs of one of the two simulations of System 3 plotted in a log-log plot. The blue squares represent the OM and the red squares the IM. The bending rigidity moduli, K_c, are fitted to the plot using values for the seven smallest wavenumbers, q, as illustrated by the straight lines. A snapshot of phosphates (grey) along the plane of the membrane at the end of the simulation is shown on the right. AcrABZ-TolC complex is shown in green, while the peripheral proteins in cyan. Similar analysis performed on System 4 (B), System 5 (C), and System 6 (D). (E) K_c values for all the systems simulated in this study. Each value is averaged over two independent simulations and error bars represent the standard deviations.

The reduced lateral diffusion of lipids around membrane proteins is discussed in detail

elsewhere,[14,15] here we focus our attention on the direction of lipid diffusion using measurements of mean square displacement (MSD) and flow analysis of the phosphate beads in each leaflet.[28] The LPS-containing leaflet of the OM displayed significantly smaller lipid motions, by around three orders of magnitude, compared to phospholipids-containing leaflets as indicated by the low MSD values (Figs 2 and S5). Similarly, our lipid flow analysis showed that all LPS moved less than 0.6 Å in the last 10 ns of the simulation compared to 1.0 to 6.0 Å for other phospholipids.

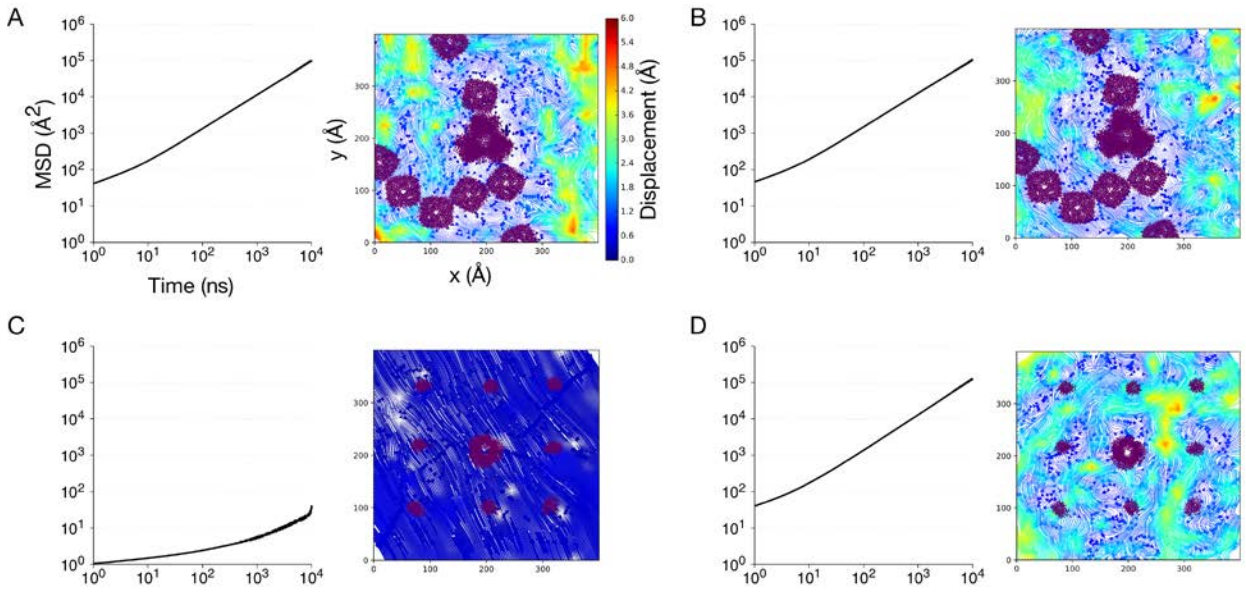

Fig 2. LPS in the OM moves significantly slower than phospholipids. (A) MSD versus time for the phospholipids in the upper leaflet of the IM of System 5 (left) and their flow averaged over the last 10 ns of the simulation (right). Arrows indicate the direction of movement of lipids, whereas the line thickness and color represent the degree of displacement. The positions of proteins in the system are mapped as purple dots. The same analyses performed for the lower leaflet of the IM (B), the upper leaflet of the OM (C), and the lower leaflet of the OM (D).

All LPS molecules in the upper leaflet of the OM diffused in the same direction in a given time frame of the flow analysis (shown by the uniform arrows in Fig 2C). This is unique to LPS as phospholipids moved randomly with no correlation between adjacent lipids. The sugar moieties in the head group of neighboring LPS molecules are cross-linked with each other via Ca^{2+} ions. The upper leaflet of the OM therefore is a strongly interconnected network of LPS molecules, which could explain why they all flow in unison. The diffusion of LPS also occurred in the same direction as OmpA and TolC, whereas in the lower leaflet of the OM phospholipids moved in random directions (Fig 3). Such correlation between protein and LPS motion is preserved even in simpler systems with smaller membranes and single proteins (Fig S6). Ca^{2+} ions are essential in maintaining the correlated motion between all LPS molecules, and in turn, between LPS and proteins. We performed some additional simulations in which we reduced the charge on the divalent cations from +2 to +1.5 *e* and found that the concerted movement was reduced, resulting in random flow similar to that observed for phospholipids in the lower leaflet (Fig. S7), thereby highlighting the important role of the divalent ions.

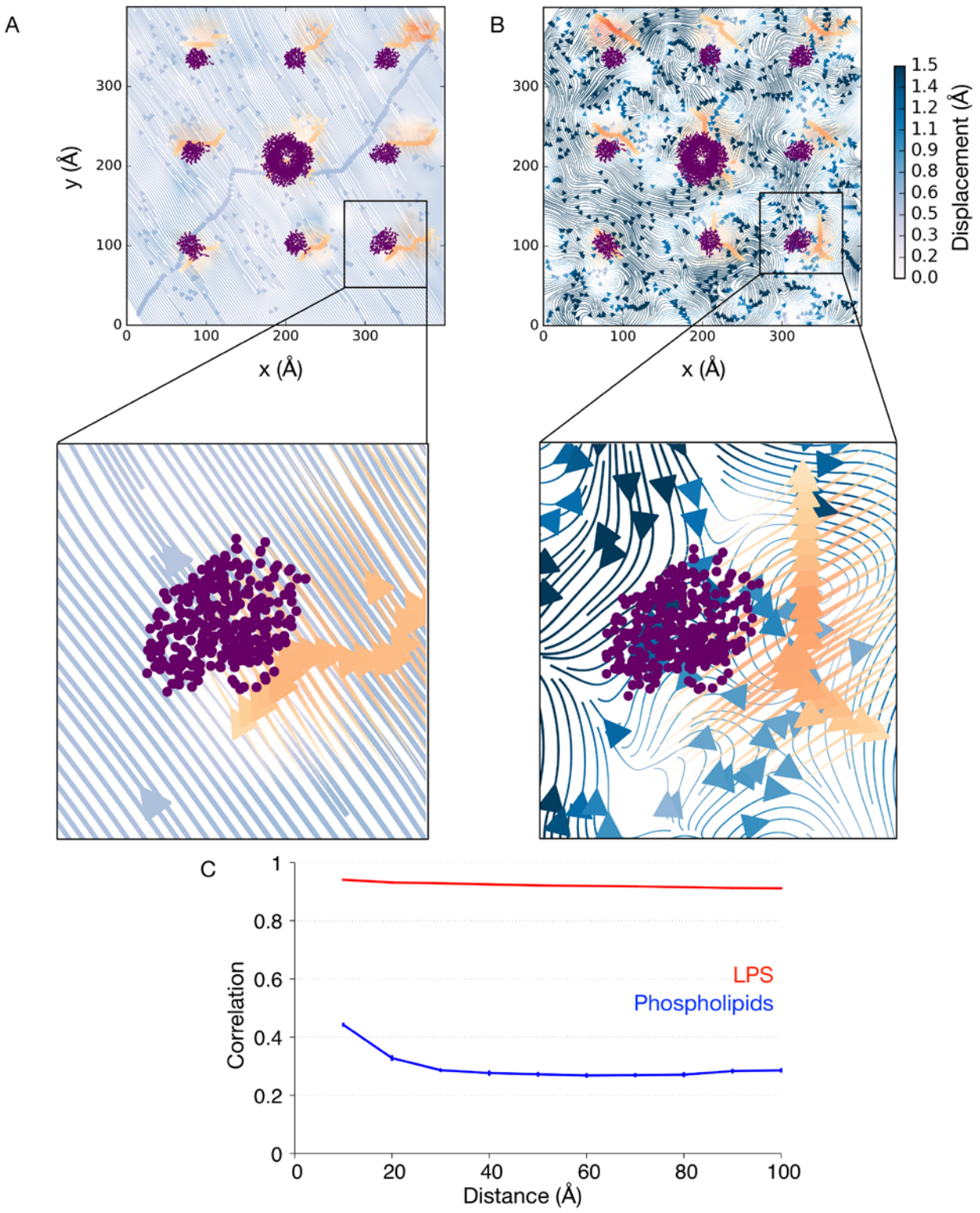

Fig 3. Concerted movement of protein and LPS in the OM. (A) The flows of lipids and proteins shown respectively in blue and orange, for the upper leaflet of the OM. Enlarged image

highlights the unidirectional motion of protein and LPS around it. (B) Same analysis on the lower leaflet of the OM. (C) Correlation between the direction of motion of lipids and proteins versus distance from the protein surface averaged over two simulations of System 5. Error bars indicate standard deviations.

There is an increasing evidence that the presence of proteins within a membrane can result in lipid sorting due to the propensity of proteins to interact with certain species of lipid.[29,30] To explore this, the ratio of contacts made by each lipid species with AcrBZ throughout the entire 10 μs simulations was compared to their initial configurations. In System 6 (eight copies of LacY), there was a remarkable enrichment of cardiolipin around AcrBZ, whereby at the end of the simulations there were around four to six times more cardiolipins than the initial configuration (Fig 4A). A density plot showed a significantly higher density of cardiolipin around AcrBZ compared to the area further away from the protein (Fig 4B). However similar enrichment was not observed for PE and PG lipids (Fig S8), the ratio of which remained the same around the proteins throughout the simulations, despite the membrane containing a higher number of these lipid types.

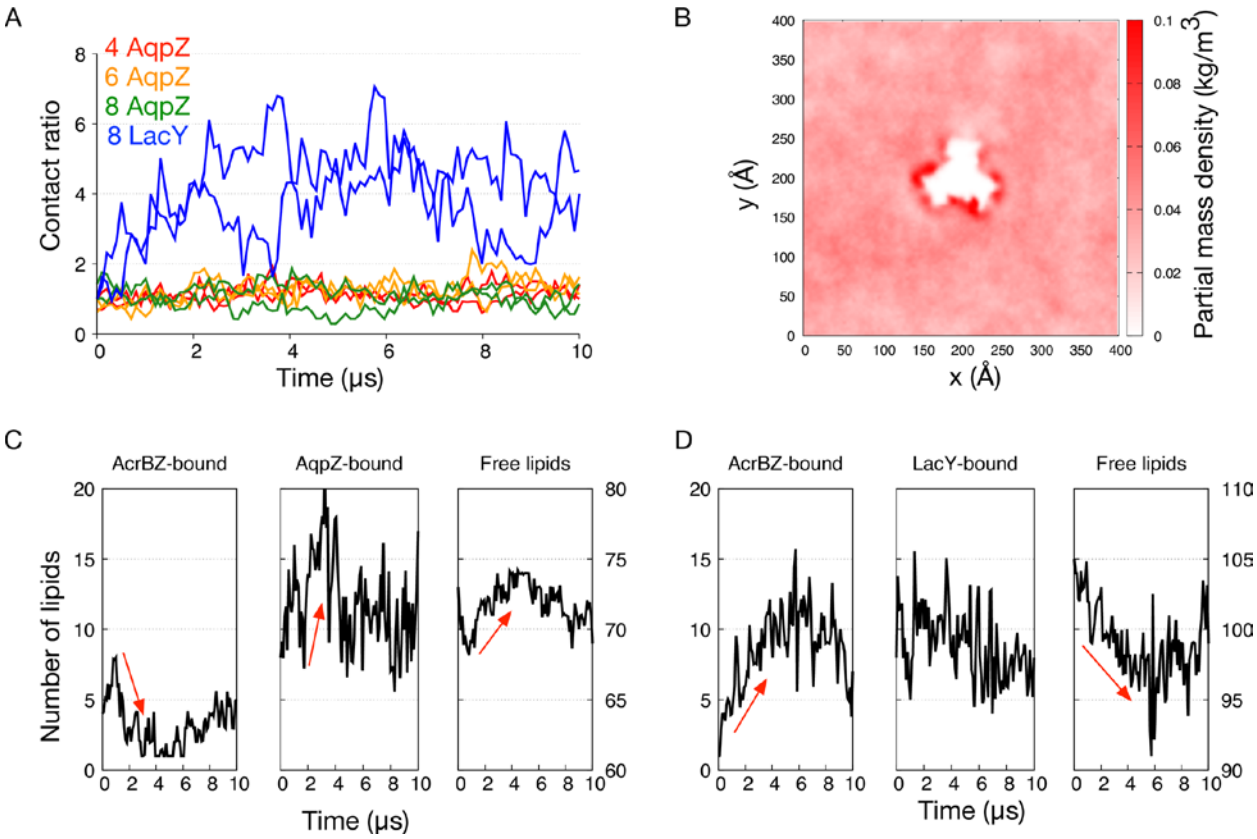

Fig 4. Cardiolipin enrichment around AcrBZ and AqpZ. (A) Contact ratio calculated as the number of cardiolipin found within 6 Å from AcrBZ complex during the entire 10 μs simulations divided by the original number at the beginning of the simulation. (B) Average density of cardiolipin in the IM of System 6. The white space in the middle of the graph indicates the position of AcrBZ. (C) The number of cardiolipin found within 10 Å from AcrBZ (left), within 10 Å from AqpZ (middle), and not within 10 Å from either protein (right) in System 5. Red arrows indicate the time point when several cardiolipins moved away from AcrBZ into the free lipids zone, before making contacts with AqpZ. (D) Similar analysis performed for System 6 to show that most cardiolipins that interacted with AcrBZ originated as free lipids, while the number of cardiolipins around LacY remained largely unchanged.

Intriguingly there was a slight decrease in the number of cardiolipins around AcrBZ during the

simulations of System 5 with eight AqpZ. A mass spectrometry study showed that AqpZ is stabilized by cardiolipin and the functioning of the protein is modulated by this lipid.[30] It therefore seems likely that the vast majority of cardiolipins in this system might preferentially interact with AqpZ during the simulations, leaving fewer cardiolipins to interact with AcrBZ. To quantify cardiolipin movement from one protein to another, we measured the number of lipids within 10 Å to both AcrBZ and AqpZ, and those that are not within 10 Å to either protein, the latter are essentially free lipids (Fig 4C). We found that after 1.0 μs the number of cardiolipin bound to AcrBZ decreased, followed by a concomitant increase in the number of free cardiolipins, and afterwards an increase the AqpZ-bound cardiolipin. At 4.0 μs the number of cardiolipins interacting with AqpZ decreased, leading to an increase in free cardiolipins in the system. This analysis suggests that cardiolipins in the system were constantly exchanged between AcrBZ and AqpZ as they were both prone to binding to this lipid. A similar analysis to LacY in System 6 revealed no change in the number of cardiolipin bound to this protein, along with a dramatic decrease in free cardiolipins and increase in the AcrBZ-bound ones (Fig 4D). This result indicates that in the presence of proteins, which bind lipids non-selectively such as LacY, cardiolipins will aggregate around other proteins that show preference towards them, further corroborating the concept of protein-induced lipid sorting.

A limitation of the current study is the omission of the peptidoglycan cell wall, which is present in the periplasmic space of the *E. coli* cell envelope. This is due to the lack of available coarse-grained models for peptidoglycan. While simulations of peptidoglycan alone or with the outer membrane has been performed at atomistic resolution,[24,31] MARTINI parameters are not currently available. For the purposes of studying the behavior of the two membranes, using an aqueous space between the two membranes, which are separated by the efflux pump is an

appropriate model.

In summary, we uncover details of the dynamical behavior of both the IM and OM as well as several crucial bacterial proteins including the multi-drug efflux pump AcrABZ-TolC complex. Our results clearly demonstrate that the movement of bacterial membranes and the flow of individual lipids within them are influenced by various different factors, most notably the surrounding integral membrane proteins. We show that some bacterial membrane proteins induce lipid sorting while others do not. Combining our results with recent experimental studies, it is abundantly clear that bacterial membrane proteins and lipids are complex, have their own individual characteristics, and still require structural, dynamic, experimental and computational study to understand how they contribute to the functioning of the cell envelope as a whole.

Computational Methods

The IM and OM were initially constructed and equilibrated separately based on the lipid composition of *E. coli* K12.[2,32–34] Both membranes were assembled into the same simulation box by aligning their hydrophobic cores to the transmembrane regions of AcrABZ-TolC complex.[35] The outer membrane was embedded with either the full length OmpA dimer[22] or its monomeric N-terminal β-barrel, whilst the inner membrane was inserted with either the aquaporin AqpZ[19] or the lactose permease LacY[20] (Table 1). These systems were equilibrated for 1 μs before two independent 10 μs production runs were performed. Detailed parameters for the simulations are available in the supplementary information.

Membrane curvature was characterized by bending rigidity constants (K_c) based on the Helfrich-Canham theory[25] as described in Fowler et al.[12] Mean square displacement of lipids was calculated using the GROMACS *g_msd*[36] tool using the phosphate bead as a reference point for

each lipid. Two-dimensional protein and lipid flow analysis was performed using scripts provided by Chavent et al.[28] Protein-lipid contact analysis was performed in VMD using an in-house script.[37] The lipid partial mass density profile was generated using a modified version of the GROMACS *g_density* tool.[38]

ASSOCIATED CONTENT

Supporting Information. The following files are available free of charge. (PDF file)

AUTHOR INFORMATION

The authors declare no competing financial interests.

ACKNOWLEDGMENT

We acknowledge use of the Iridis III and IV supercomputers at the University of Southampton.

(1) Silhavy, T. J.; Kahne, D.; Walker, S. The Bacterial Cell Envelope. *Cold Spring Harb. Perspect. Biol.* **2010**, *2* (5), 1–17.

(2) Lugtenberg, E. J. .; Peters, R. Distribution of Lipids in Cytoplasmic and Outer Membranes of Escherichia Coli K12. *Biochim. Biophys. Acta* **1976**, *441* (195 6), 38–47.

(3) Höltje, J. V. Growth of the Stress-Bearing and Shape-Maintaining Murein Sacculus of Escherichia Coli. *Microbiol. Mol. Biol. Rev.* **1998**, *62* (1), 181–203.

(4) Vollmer, W.; Bertsche, U. Murein (Peptidoglycan) Structure, Architecture and Biosynthesis in Escherichia Coli. *Biochim. Biophys. Acta.* **2008**, *1778* (9), 1714–1734.

(5) Dupuy, A. D.; Engelman, D. M. Protein Area Occupancy at the Center of the Red Blood Cell Membrane. *Proc. Natl. Acad. Sci. U.S.A.* **2008**, *105* (8), 2848–2852.

(6) Takamori, S.; Holt, M.; Stenius, K.; Lemke, E. A.; Gronborg, M.; Riedel, D.; Urlaub, H.; Schenck, S.; Brugger, B.; Ringler, P.; et al. Molecular Anatomy of a Trafficking Organelle. *Cell* **2006**, *127* (4), 831–846.

(7) Koshy, C.; Ziegler, C. Structural Insights into Functional Lipid-Protein Interactions in Secondary Transporters. *Biochim. Biophys. Acta* **2014**.

(8) Dawaliby, R.; Trubbia, C.; Delporte, C.; Masureel, M.; Van Antwerpen, P.; Kobilka, B. K.; Govaerts, C. Allosteric Regulation of G Protein–coupled Receptor Activity by Phospholipids. *Nat. Chem. Biol.* **2015**, *12* (JANUARY), 35–41.

(9) Drachmann, N. D.; Olesen, C.; Møller, J. V; Guo, Z.; Nissen, P.; Bublitz, M. Comparing Crystal Structures of Ca(2+) -ATPase in the Presence of Different Lipids. *FEBS J.* **2014**,

281 (18), 4249–4262.

(10) Arnarez, C.; Mazat, J. P.; Elezgaray, J.; Marrink, S. J.; Periole, X. Evidence for Cardiolipin Binding Sites on the Membrane-Exposed Surface of the Cytochrome bc1. *J. Am. Chem. Soc.* **2013**, *135* (8), 3112–3120.

(11) Palsdottir, H.; Hunte, C. Lipids in Membrane Protein Structures. *Biochim. Biophys. Acta.* **2004**, *1666* (1–2), 2–18.

(12) Fowler, P. W.; Hélie, J.; Duncan, A.; Chavent, M.; Koldsø, H.; Sansom, M. S. P. Membrane Stiffness Is Modified by Integral Membrane Proteins. *Soft Matter* **2016**, *12* (37), 7792–7803.

(13) Koldsø, H.; Sansom, M. S. P. Organization and Dynamics of Receptor Proteins in a Plasma Membrane. *J. Am. Chem. Soc.* **2015**, *137* (46), 14694–14704.

(14) Goose, J. E.; Sansom, M. S. P. Reduced Lateral Mobility of Lipids and Proteins in Crowded Membranes. *PLoS Comput. Biol.* **2013**, *9* (4).

(15) Niemelä, P. S.; Miettinen, M. S.; Monticelli, L.; Hammaren, H.; Bjelkmar, P.; Murtola, T.; Lindahl, E.; Vattulainen, I. Membrane Proteins Diffuse as Dynamic Complexes with Lipids. *J. Am. Chem. Soc.* **2010**, *132* (22), 7574–7575.

(16) Holdbrook, D. A.; Huber, R. G.; Piggot, T. J.; Bond, P. J.; Khalid, S. Dynamics of Crowded Vesicles: Local and Global Responses to Membrane Composition. *PLoS One* **2016**, *11* (6), e0156963.

(17) Venter, H.; Mowla, R.; Ohene-Agyei, T.; Ma, S. RND-Type Drug Efflux Pumps from

Gram-Negative Bacteria: Molecular Mechanism and Inhibition. *Front. Microbiol.* **2015**, *6* (APR), 1–11.

(18) Yamaguchi, A.; Nakashima, R.; Sakurai, K. Structural Basis of RND-Type Multidrug Exporters. *Front. Microbiol.* **2015**, *6* (APR), 1–19.

(19) Jiang, J.; Daniels, B. V.; Fu, D. Crystal Structure of AqpZ Tetramer Reveals Two Distinct Arg-189 Conformations Associated with Water Permeation through the Narrowest Constriction of the Water-Conducting Channel. *J. Biol. Chem.* **2006**, *281* (1), 454–460.

(20) Abramson, J.; Smirnova, I.; Kasho, V.; Verner, G.; Kaback, H. R.; Iwata, S. Structure and Mechanism of the Lactose Permease of Escherichia Coli. *Science (80-.).* **2003**, *301* (5633), 610–615.

(21) Smith, S. G. J.; Mahon, V.; Lambert, M. A.; Fagan, R. P. A Molecular Swiss Army Knife: OmpA Structure, Function and Expression. *FEMS Microbiol. Lett.* **2007**, *273* (1), 1–11.

(22) Marcoux, J.; Politis, A.; Rinehart, D.; Marshall, D. P.; Wallace, M. I.; Tamm, L. K.; Robinson, C. V. Mass Spectrometry Defines the C-Terminal Dimerization Domain and Enables Modeling of the Structure of Full-Length OmpA. *Structure* **2014**, *22* (5), 781–790.

(23) Ortiz-Suarez, M. L.; Samsudin, F.; Piggot, T. J.; Bond, P. J.; Khalid, S. Full-Length OmpA: Structure, Function, and Membrane Interactions Predicted by Molecular Dynamics Simulations. *Biophys. J.* **2016**, *111* (8), 1692–1702.

(24) Samsudin, F.; Ortiz-Suarez, M. L.; Piggot, T. J.; Bond, P. J.; Khalid, S. OmpA: A Flexible

Clamp for Bacterial Cell Wall Attachment. *Structure* **2016**, *24* (12), 2227–2235.

(25) Helfrich, W. Elastic Properties of Lipid Bilayers: Theory and Possible Experiments. *Z Naturforsch C* **1973**, *28* (11), 693–703.

(26) Zhong-Can, O.-Y.; Helfrich, W. Instability and Deformation of a Spherical Vesicle by Pressure. *Phys. Rev. Lett.* **1987**, *59* (21), 2486–2488.

(27) Grouleff, J.; Søndergaard, S.; Koldsø, H.; Schiøtt, B. Properties of an Inward-Facing State of LeuT : Conformational Stability and Substrate Release. *Biophys. J.* **2015**, *108* (6), 1390–1399.

(28) Chavent, M.; Reddy, T.; Goose, J.; Dahl, A. C. E.; John, E.; Jobard, B.; Sansom, M. S. P. Methodologies for the Analysis of Instantaneous Lipid Diffusion in MD Simulations of Large Membrane Systems. *Faraday Discuss.* **2014**, *169*, 455–475.

(29) Kalli, A. C.; Sansom, M. S. P.; Reithmeier, R. A. F. Molecular Dynamics Simulations of the Bacterial UraA H+-Uracil Symporter in Lipid Bilayers Reveal a Closed State and a Selective Interaction with Cardiolipin. *PLoS Comput. Biol.* **2015**, *11* (3), 1–27.

(30) Laganowsky, A.; Reading, E.; Allison, T. M.; Ulmschneider, M. B.; Degiacomi, M. T.; Baldwin, A. J.; Robinson, C. V. Membrane Proteins Bind Lipids Selectively to Modulate Their Structure and Function. *Nature* **2014**, *510* (7503), 172–175.

(31) Gumbart, J. C.; Beeby, M.; Jensen, G. J.; Roux, B. Escherichia Coli Peptidoglycan Structure and Mechanics as Predicted by Atomic-Scale Simulations. *PLoS Comput. Biol.* **2014**, *10* (2).

(32) Aibara, S.; Kato, M.; Ishinaga, M.; Kito, M. Changes in Positional Distribution of Fatty Acids in the Phospholipids of Escherichia Coli after Shift-Down in Temperature. *Biochim. Biophys. Acta* **1972**, *270*, 301–306.

(33) Kito, M.; Ishinaga, M.; Nishihara, M.; Kato, M.; Sawada, S. Metabolism of the Phosphatidylglycerol Molecular Species in Escherichia Coli. *Eur. J. Biochem.* **1975**, *54* (1), 55–63.

(34) Yokota, K.; Kanamoto, R.; Kito, M. Composition of Cardiolipin Molecular Species in Escherichia Coli. *J. Bacteriol.* **1980**, *141* (3), 1047–1051.

(35) Du, D.; Wang, Z.; James, N. R.; Voss, J. E.; Klimont, E.; Ohene-Agyei, T.; Venter, H.; Chiu, W.; Luisi, B. F. Structure of the AcrAB-TolC Multidrug Efflux Pump. *Nature* **2014**, *509* (7501), 512–515.

(36) Hess, B.; Kutzner, C.; Spoel, D. V. D. GROMACS 4: Algorithms for Highly Efficient, Load-Balanced, and Scalable Molecular Simulation. *J. Chem. Theory Comput.* **2008**, *4* (3), 435–447.

(37) Humphrey, W.; Dalke, A. VMD: Visual Molecular Dynamics. *J. Mol. Graph.* **1996**, *15*, 33–38.

(38) Castillo, N.; Monticelli, L.; Barnoud, J.; Tieleman, D. P. Free Energy of WALP23 Dimer Association in DMPC, DPPC, and DOPC Bilayers. *Chem. Phys. Lipids.* **2013**, *169*, 95–105.